

Presented at the ASHRAE Winter Meeting, Atlanta, GA,  
February 17–21, 1996, and to be published in the Proceedings

**A Comparison Between Calculated and Measured  
SHGC for Complex Fenestration Systems**

**J.H. Klems, J.L. Warner, and G.O. Kelley**

September 1995

Prepared for the U.S. Department of Energy under Contract Number DE-AC03-76SFOO098

#### **DISCLAIMER**

This document was prepared as an account of work sponsored by the United States Government. While this document is believed to contain correct information, neither the United States Government nor any agency thereof, nor The Regents of the University of California, nor any of their employees, makes any warranty, express or implied, or assumes any legal responsibility for the accuracy, completeness, or usefulness of any information, apparatus, product, or process disclosed, or represents that its use would not infringe privately owned rights. Reference herein to any specific commercial product, process, or service by its trade name, trademark, manufacturer, or otherwise, does not necessarily constitute or imply its endorsement, recommendation, or favoring by the United States Government or any agency thereof, or The Regents of the University of California. The views and opinions of authors expressed herein do not necessarily state or reflect those of the United States Government or any agency thereof, or The Regents of the University of California.

Ernest Orlando Lawrence Berkeley National Laboratory  
is an equal opportunity employer.

Presented at the ASHRAE Winter Meeting, Atlanta, GA, February 17-21, 1996, and published in the Proceedings.

## **A Comparison Between Calculated and Measured SHGC for Complex Fenestration Systems**

J. H. Klems, J. L. Warner, and G. O. **Kelley**  
Building Technologies Program  
Energy and Environment Division  
Lawrence Berkeley National Laboratory  
University of California  
Berkeley, CA 94720

September 1995

This research was jointly supported by ASHRAE, as Research Project **548-RP** under Agreement No. BG 87-127 with the U.S. Department of Energy, and by the Assistant Secretary for Energy Efficiency and Renewable Energy, Office of Building Technologies, Building Systems and Materials Division of the U.S. Department of Energy under Contract No. DE-AC03-76SF00098.

# A Comparison Between Calculated and Measured SHGC for Complex Fenestration Systems

J. H. **Klems**, J. L. Warner, and G. O. **Kelley**  
Building Technologies Program  
Energy and Environment Division  
Lawrence Berkeley National Laboratory  
University of California  
Berkeley, CA 94720

## ABSTRACT

Calorimetric measurements of the dynamic net heat flow through a complex fenestration system consisting of a buff venetian blind inside clear double glazing are used to derive the **direction-**dependent beam SHGC of the fenestration. These measurements are compared with calculations according to a proposed general method for deriving complex fenestration system **SHGC's** from bidirectional layer optical properties and generic calorimetric properties. Previously published optical measurements of the same venetian blind and generic inward-flowing fraction measurements are used in the calculation. The authors find satisfactory agreement between the SHGC measurements and the calculation.

Significant dependence on incident angle was found in the measured **SHGC's**. Profile angle was not found to be a useful variable in characterizing the system performance. The predicted SHGC was found to be inherently dependent on two angles, although only the incident angle variations were observable under the test conditions.

## INTRODUCTION

This paper is the last in a series of five publications summarizing work on the joint ASHRAE/DOE Research Project **548-RP**. The goal of this research project was to develop a method for characterizing the performance of fenestration systems containing optically complex elements, such as venetian blinds, shades, or other nonsecular shading devices, and to demonstrate the feasibility of this method by accumulating the data necessary to apply the method and comparing the resulting prediction of solar heat gain coefficient (**SHGC**) with measurements made under realistic conditions.

The first publication (**Klems 1994A**) outlines the general strategy, physical basis, and mathematics of the method. Beginning with the standard definition of the SHGC,  $F$ , extension to a **multilayer** complex fenestration system requires an  $F$  that may depend (in the most complex case) on **two angles ( $\theta, \phi$ ) specifying the incoming direction. The incident angle,  $\theta$ , is the angle between the incident rays and the normal to the plane of the glazings. When one of the fenestration elements has a characteristic direction in the glazing plane (e.g., the direction of venetian blind slats), then  $F$  may also depend on the azimuthal angle,  $\phi$ , of the plane of incidence (the plane containing both the incident direction and the normal to the glazing plane) relative to that characteristic direction. In the general case, then, the SHGC is given by**

$$F(\theta, \phi) = T_{fH}(\theta, \phi) + \sum_{i=1}^M N_i A_{fi}(\theta, \phi), \quad (1)$$

where  $T_{fH}$  is the directional-hemispherical solar-optical transmittance of the system, it is assumed that there are  $M$  layers,  $A_{fi}$  is the front absorption and  $N_i$  the inward-flowing fraction (**IFF**) of the  $i$  th layer. For determining  $F$  the project methodology utilizes two strategies, which we term *thermal-solar separation* and the *layer method*: (1) *Thermal-solar separation*:  $N_i$  must be determined calorimetrically for a given system geometry and set of **emittances**, but will be the same for all such systems regardless of the solar-optical properties of the layers. It therefore need only be determined once for a “thermally prototypic” system and can be combined with quantities  $T_{fH}$  and  $A_{fi}$  determined by non-calorimetric optical techniques to produce values of  $F$  for a variety of similar systems. The fourth publication (**Klems and Kelley 1995**) presents the results of an extensive set of calorimetric measurements of layer-specific inward-flowing fractions for common thermally prototypic systems involving shading. (2) *The layer method*:  $T_{fH}$  and  $A_{fi}$ , which are system **solar-optical properties** ( $A_{fi}$  being the layer absorptance in a given system), are calculated from the bi-directional transmittance and reflectance distribution functions of individual layers.

In addition the project characterizes complex layer hi-directional properties by a measurement of their spatially-averaged characteristics over a suitably chosen grid of discrete directions. The second publication (**Klems 1994B**) describes how this is done, develops the detailed mathematical formulas that result for calculating  $T_{fH}$  and  $A_{fi}$  from the discretized bidirectional layer properties, and works out a simple example calculation. The third publication (**Klems and Warner 1995**) describes the method of making the layer bidirectional measurements, utilizing the LBL Scanning **Gonio-Radiometer/Photometer Facility** (“scanner”), and presents measurements made on a white diffusing shade and on a buff venetian blind with slats tilted at a 45° angle relative to the plane of the blind.

This paper is concerned with validating the method by comparing (a) the value of  $F$  obtained from equation 1 and the separate measurements of bidirectional layer properties and layer-specific inward-flowing fractions with (b) direct measurements of  $F$  utilizing dynamic calorimetry. Because the focus of the whole effort is on a methodology that will be useful for predicting dynamic fenestration heat flows in buildings, we chose to make the measurements under conditions that reflect the field conditions under which windows with shading systems might be used.

A preliminary paper (**Klems and Warner 1992**) had shown that the method is valid for the white diffusing shade inside clear double glazing. This is not a very stringent test of the method. The shade has low transmittance and the diffuse nature of its reflectance washes out most **angular** dependence of the glazings. It was generally recognized that a venetian blind presents a much more demanding test. We treat this case in the present paper.

## THE MOWITT FACILITY

SHGC'S were measured using a well-known mobile thermal test facility (**Klems, Selkowitz et al. 1982; Klems 1988**) in **Reno, NV**. This is a mobile calorimetric facility designed to measure the net heat flow through a fenestration as a function of time under realistic outdoor conditions. Consisting of dual, guarded, room-sized calorimeters in a mobile structure, the it can simultaneously expose two

windows to a room-like interior environment and to ambient outdoor weather conditions while accurately measuring the net heat flow through each window. This measurement comes from a net heat balance on each calorimeter chamber, performed at short intervals. To get an accurate net heat balance measurement and control the interior air temperature during the full diurnal cycle, each calorimeter chamber contains an electric heater, a liquid-to-air heat exchanger with measured flow rate and inlet/outlet temperatures, and a nearly continuous interior skin of large area heat flow sensors. There are also provisions for measuring all auxiliary electric power dissipated inside the chambers (e.g., fan power). A diagram and photograph of the facility can be found in (Klems and Kelley 1995).

During the measurement associated instrumentation measures a variety of internal and external conditions: An array of thermistors with radiation shields monitors the average interior air temperature in each calorimeter, and an aspirated thermistor located in the on-site weather tower measures the exterior air temperature. A standard rotating-cup anemometer and weather vane measures the free-stream wind speed and direction. A sun-tracking **pyrheliometer** and a horizontally-mounted pyranometer measures beam and total horizontal solar intensity, respectively. A vertically-mounted pyranometer mounted above the two window samples measures the total solar (and ground-reflected) radiation intensity incident on the windows, and a vertically-mounted pyrgeometer measures the total incident long-wave infrared radiation (emitted by the sky and ground). A specially-designed sensor located between the two window samples monitored the nighttime effective heat transfer film coefficient.

#### MOWITT MEASUREMENT OF SOLAR HEAT GAIN COEFFICIENTS

Direction-dependent **SHGC's** were derived from the measured net heat flow through the fenestration systems using the following model:

$$W(t) = A \cdot [T_o(t) - T_i(t)] + B_D \cdot g_0(t) \cdot I_D(t) + \left[ \sum_{n=1}^6 B_n \cdot g_n(t) \right] \cdot I_B(t) \cdot \cos(\theta(t)), \quad (2)$$

where A, **B<sub>D</sub>** and **B<sub>n</sub>** are fitted constants and the functions  $g_0$  and  $g_n$  are defined as

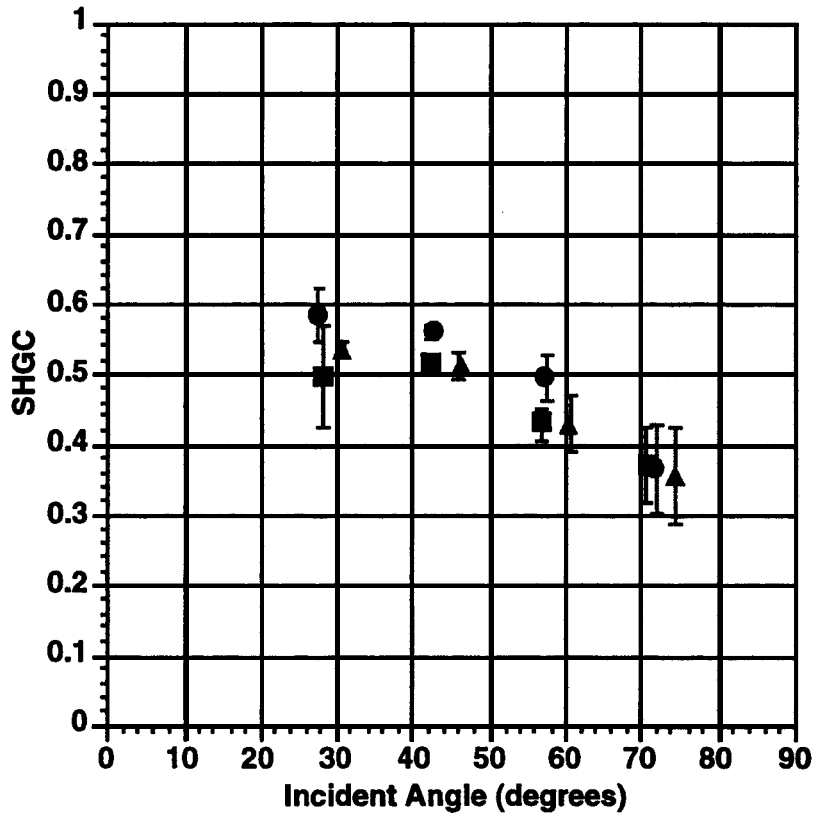
$$g_0(t) = \begin{cases} 1 & \text{if the sun is up at time } t \\ 0 & \text{otherwise} \end{cases} \quad (3)$$

$$g_n(t) = \begin{cases} 1 & \text{if } t \text{ is within hour } n \\ 0 & \text{otherwise} \end{cases}$$

window-afternoon hours in most cases, since the orientation was west-facing. When there were not six hours of daylight, terms were dropped from the sum and the corresponding B values ignored in the fitting.

This fitting procedure yielded for the  $B_n$  hourly average values of  $\langle F(\theta, \phi) \rangle \cdot A_G$ , where  $A_G$  is the glazed area of the fenestration. By separately averaging the solar angles over the same hourly intervals, we could associate the  $B_n$  with the corresponding average sun angles. Because the sun angles may change on the order of  $15^\circ$  per hour, this procedure gave the determination an angular resolution comparable to that of the scanner measurements.

For the case of the buff venetian blind (for which scanner measurements are described in (Klems and Warner 1995)) mounted as an interior blind on a wood-frame, double-glazed window (2.5 mm clear glass each pane), the derived beam solar heat gain coefficients are plotted in Figure 1



reasonably well, even though the solar azimuths of data points with the same incident angle may be substantially different. This point will be discussed further below. Differences between measurements may also reflect the difficulty of setting the blind slats at a precisely reproducible tilt angle in the field. Points in the plot are untrustworthy at both extreme high and low incident angles. The high angles occurred just after solar noon when the sun begins to be incident on the west-facing facade; these conditions are particularly sensitive to window reveal, exact placement of the blind relative to the window frame, and other idiosyncracies of the experiment. Low angles, on the other hand, occurred near sunset and correspond to low solar intensity. Errors in heat flow measurement, small residual time lags in the chamber, and similar effects combine to make these points less reliable than the plotted error bars (which are derived from the fitting uncertainty) indicate. In addition, the particular fit method used may produce underestimates of the true uncertainty, since certain correlations between the fitted parameters were disallowed in order to avoid predictable experimental problems. For example, hours when there was direct sun were not allowed to contribute to the fitting of the diffuse constant.

A comparison of the measured data from the MoWiTT and the model of equation 2 is given for one day in Figure 2. A histogram-like solid line at the bottom of the peak indicates schematically

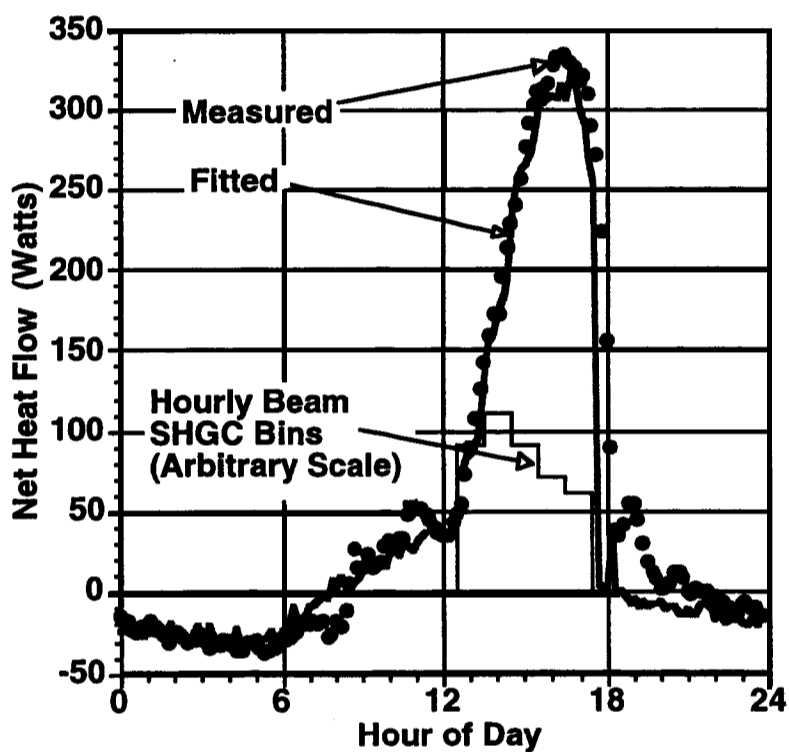


*Figure 2. Measured and Fitted Net Heat Flows Through a Double Glazed Window with Interior Buff Venetian Blind at 45° Slat Tilt. Measurements of the net heat flowing through the fenestration system, made every 10 minutes by the MoWiTT calorimeter (points), are*



the time intervals over which the beam SHGC is assumed to be constant in the fit (by means of the  $g_n$  functions). As can be seen from the figure, the fit is reasonably good for most of the bins of beam irradiation; however, for the last one there is a significant departure between model and data. In general, we find that equation 2 is not an adequate form for modeling the data in the region near and immediately after local sunset. While there may be a number of reasons for this, the immediate implication is that the parameter obtained in the fit for that time does not have the intended physical meaning, and we have accordingly discarded the last fitted constant. Similarly, it can be seen that in the region before noon the curve, while fitting the data on the average, does not have the same shape as the data. This would imply that the fitted value for  $B_0$  should not be interpreted as the **area-weighted hemispherical-averaged SHGC**, and that a more careful model of the diffusely-incident solar energy must be constructed in order to obtain fitted parameters that can be calculated from the scanner measurements. Accordingly, in Table 1 we display only beam SHGC's from the first (i.e., leftmost) four bins indicated in Figure 2.

**Table 1. MoWiTT Measurements and Layer Calculation of the Solar Heat Gain Coefficient for Clear Double Glazing with an Interior Venetian Blind, Slat Angle 45° Down**

<b>Measurement Run</b>	<b>Mean Solar Incident Direction</b>		<b>SHGC</b>	
	<b><math>\theta</math> (degrees)</b>	<b><math>\phi-180</math> (degrees)</b>	<b>MoWiTT Measurement</b>	<b>Layer Calculation</b>
Ott, 1988	28.29	159.03	0.49 * 0.07	0.59
	42.48	149.84	0.51 * 0.01	0.52
	56.77	145.73	0.43 * 0.02	0.45
	70.77	143.87	0.37 * 0.05	0.25
August, 1989	30.90	111.89	0.53 * 0.01	0.52
	46.07	117.10	0.51 * 0.02	0.48
	60.58	119.31	0.43 * 0.04	0.40
	74.47	120.03	0.35 * 0.07	0.22
Sept, 1991	27.56	132.69	0.58 ± 0.04	0.54
	42.57	131.60	0.56 ± 0.01	0.50
	57.54	131.27	0.49 ± 0.03	0.43
	71.84	130.94	0.37 ± 0.06	0.27

It has sometimes been suggested that the profile angle is the important variable in characterizing the performance of fenestration systems with venetian blinds. In Figure 3 we plot the same fitted hourly solar heat gain coefficients as functions alternatively of incident angle and profile angle. As can be seen, the data cluster much less closely when plotted versus profile angle, indicating that the latter has no special role in predicting performance, beyond determining whether there is admission of direct sunlight.

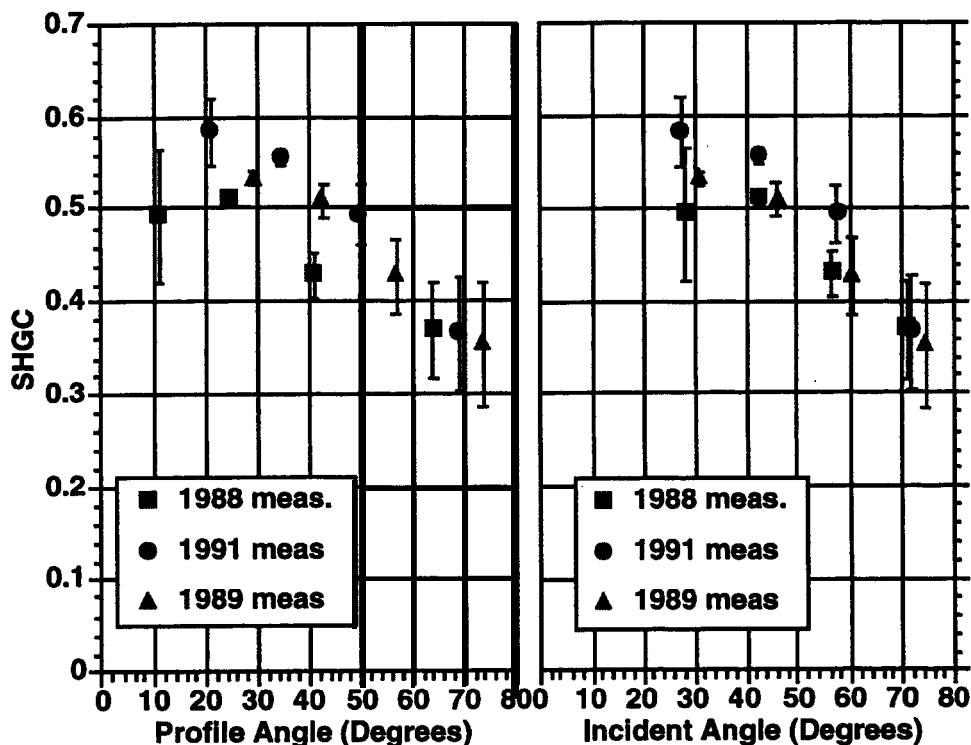
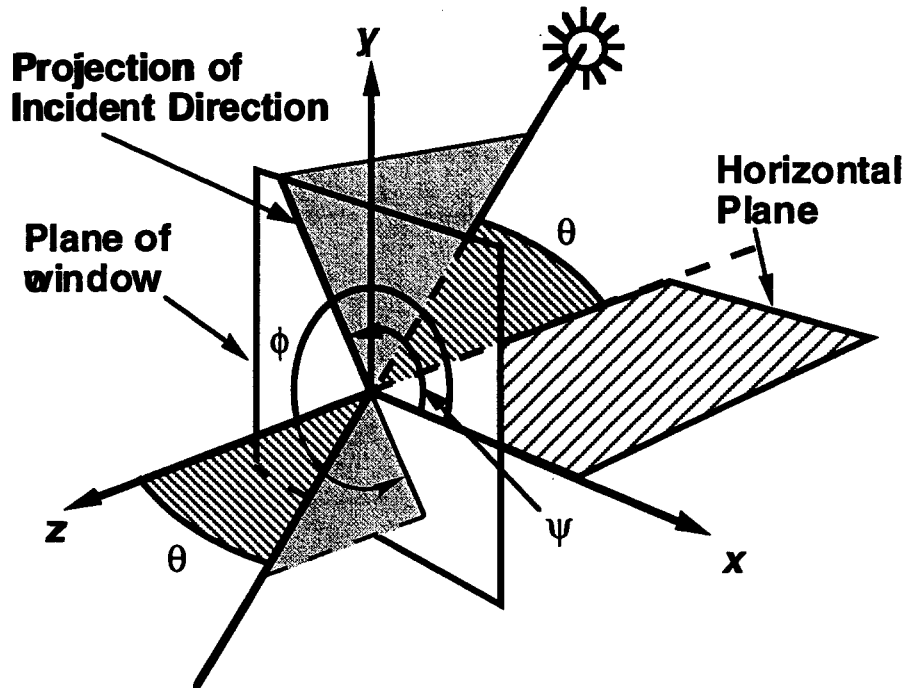


Figure 3. Profile vs Incident Angle as Independent Variable, Clear Double Glazing with Interior Buff Blind at 45° Downward Slant Tilt. Three sets of MoWiTT measurements of beam SHGC's made at different times involve different sun trajectories, and hence different combinations of incident angle and projected azimuth. When the points are plotted versus profile angle, left, the separate measurements appear to follow separate trajectories, while when they are plotted versus incident angle, right, all three measurements appear to cluster (within experimental error bars) around a common curve.

#### COMPARISON OF THE LAYER CALCULATION WITH MOWITT MEASUREMENTS

The scanner measurements of  $\tau^f(\theta_o, \phi_o; \theta_i, \phi_i)$ ,  $\rho^f$ ,  $\tau^b$  and  $\rho^b$  discussed in (Klems and Warner 1995) for the buff venetian blind with 45° slat tilt together with published (Rubin 1985) properties of clear glazing were utilized in the layer calculation method described in (Klems 1994A) to produce the directional-hemispherical transmittance and system directional layer **absorptances** for double glazing with interior blind. The layer calculations were carried out on the 15° angular grid of Figure 3 of (Klems 1994A). These were in turn combined with the results for  $N_i$  from Table 1 of (Klems

and Kelley 1995) using equation 2 of (Klems 1994A) and (Klems 1994B) to produce the beam solar heat gain coefficient,  $F(\theta, \phi)$ . The angle  $\phi$ , which was defined in (Klems 1994A) for the layer coordinate systems, is inconvenient when discussing sun angles. We use instead the angle  $\psi$ , where  $\psi = \phi - 180^\circ$ . The angle  $\theta$  retains its identity as the angle of incidence. The relation of these angles to the sun direction is shown in Figure 4. The resulting function of two angular variables is displayed in Figure 5 for downward-going incident directions.



**Figure 4.** Relation Between Sun Angles ( $\theta, \psi$ ) and Layer Coordinates ( $\theta, \phi$ ).

The calculation in Figure 5 is based on the photometric data accumulated by the scanner. A second calculation was also carried out using **radiometric** (spectrally flat) sensor data. In principle, the latter is preferable; however, in this instance a number of problems made the **radiometric** data suspect. First, the low transmission of the blind in the forward direction meant a low radiometer signal in that sensor, which because it is a thermal sensor is much less sensitive than the photometric. For the photometric sensor internal noise is negligible; for the radiometric sensor it was a serious problem. The sensor was also vulnerable to thermal drifts, and we had some indication that there was heating of the sensor and integrating sphere in angular configurations for which there was higher transmittance, and this in turn may have caused thermal drifts that were significant when the detector moved to a region of smaller transmittance. Since we do not expect a great deal of spectral selectivity between the visible and near-infrared regions for this venetian blind, the authors are inclined to believe the photometric sensor when the two disagree.

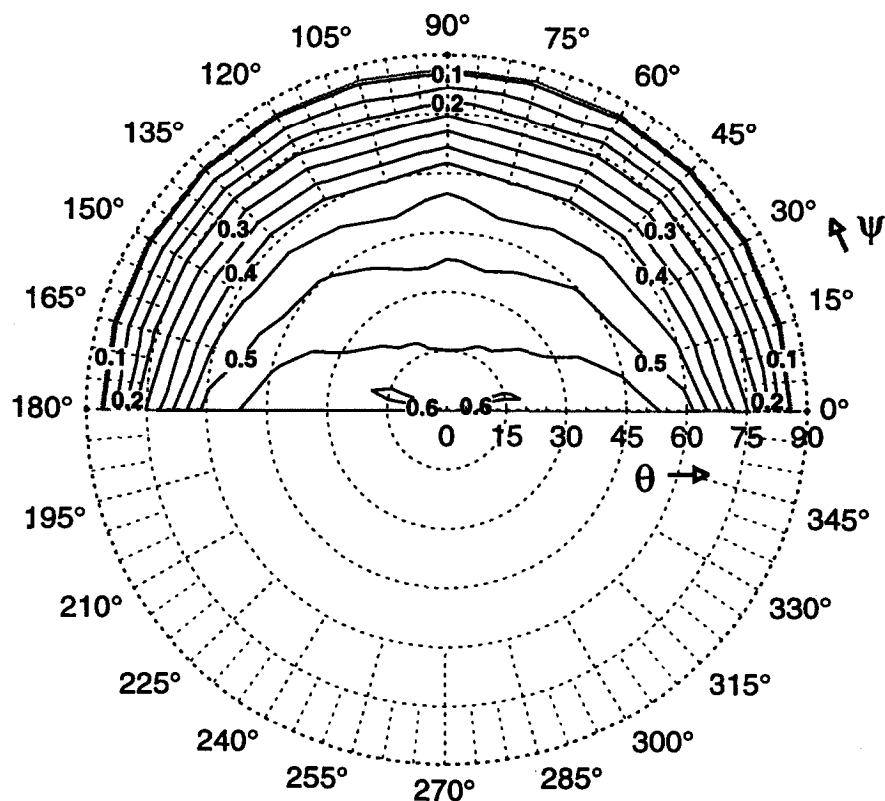


**Figure 5. Calculated Solar Heat Gain Coefficient.** Utilizing the layer method, the measured bidirectional photometric properties and inward-flowing fractions were utilized to calculate the directional solar heat gain coefficient (for downward-sloping incident directions), which is displayed here as contours of constant SHGC plotted in a polar plot where the radius is the incident angle,  $\theta$ , and the azimuth is the incident azimuthal direction,  $\psi$ .

In Figure 5 the solar heat gain coefficient is shown only for downward-sloping incident directions ( $f-p \leq 0$ ). Upward-sloping incident directions can occur only for ground-reflected radiation, which is a broad angular distribution because the reflection is diffuse. Ground-reflected radiation will appear as a part of the diffuse component of the incident solar intensity, which at least on clear days is much smaller than the beam contribution. In the following we will be discussing primarily beam radiation. The transmittance for upwardly-sloping incidence does appear as part of the solar heat gain coefficient for downward incidence, but the radiation must first undergo at least two reflections, one from the blind and the other from the pair of glass layers. Since the blind reflectance is **non**-secular and the reflectance of the glass system is low, the upward-going intensity incident on the blind will be low; hence, small variations in the transmittance for upward-going radiation will not affect the overall system transmittance appreciably. For this reason, we conserved measurement time by deriving the upward-incident front transmittance of the system from the downward-incident back transmittance measurements, which by assuming front-back blind symmetry neglects the effects of slat curvature. We do not expect that appreciable errors are introduced by this assumption,

As can be seen from Figure 5, variation of  $F(\theta, \phi)$  is much stronger with  $\theta$  than with  $\phi$ , which made it meaningful to plot the data as in Figure 1. The actual MoWiTT measurements from which this graph is drawn are listed in Table 1, from which it can be seen that the overall variation in  $\phi$  is substantial, however, and a quantitative comparison between the measurement and calculation must take this into account. Figure 6 illustrates how this was done; it shows the approximate sun

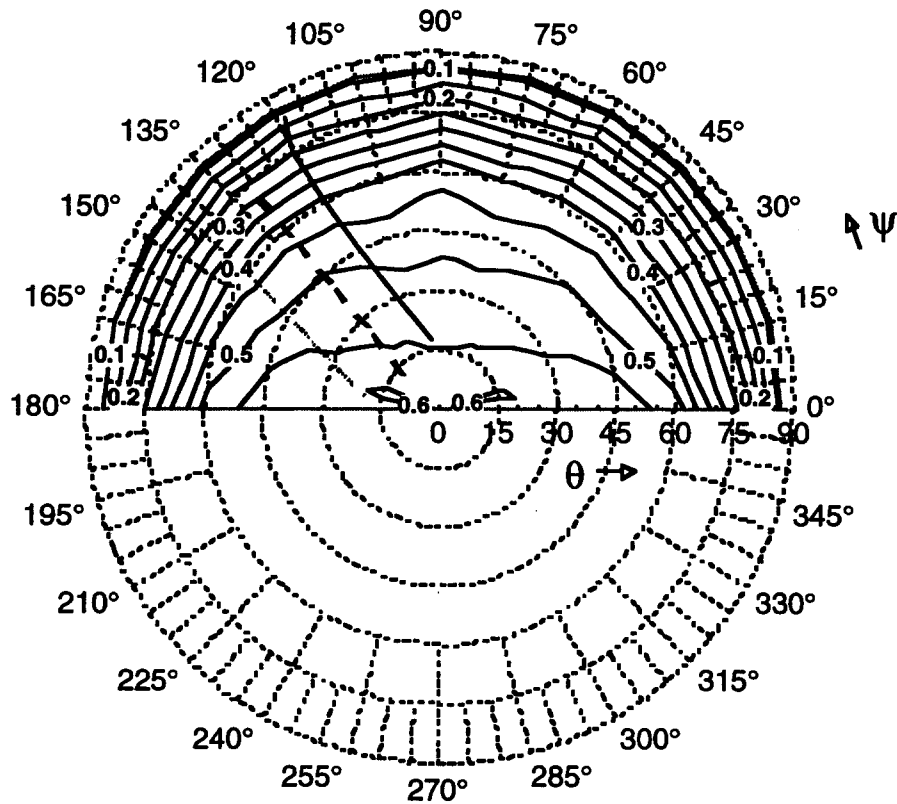


Figure 6. Averaged Sun Trajectories of the MoWiTT Measurement Periods Compared with Calculated Directional SHGC for the Buff Venetian Blind at a 45° (sun-excluding) Slat Angle. Heavy solid line: August 1989 period; heavy dashed line: September 1991 period; light dotted line: October 1988 period

trajectories, expressed in the  $[\theta, \psi$  (or  $\phi)]$  coordinates, for the three measurement periods displayed in Table 1 and Figure 1. These trajectories make clear why it is possible to plot the data, which clearly has some bivariate dependence in figure 5, as a function of the single variable  $\theta$  in Figure 1: all three sun trajectories almost lie along a  $\psi$ =constant line, and are also nearly perpendicular to the  $F$ =constant contours. This means that for all three measurement periods  $F$  is approximately the same function of  $\theta$ , with small differences between the measurement periods emerging for ( $\theta$  below 45°). As mentioned previously, the layer calculation was carried out on a 15° angular net, producing ultimately values on  $F(\theta, \phi)$  over the same net. Values at the measured directions (which lie on the appropriate trajectories in Figure 6) were then obtained by double linear interpolation of the calculated values. The interpolated values appear in the rightmost column of Table 1 and are based on the photometric data for the blind.

In Figure 7 we compare each of the three data sets to the corresponding layer calculation interpolated to the correct incident directions. All of the data in this plot is taken from Table 1. Each set of points must be compared only to its corresponding curve, which is drawn from the appropriate trajectory in Figure 6; for example, the 1989 data fits its curve more closely than do either of the other two data sets; the fact that the 1991 curve lies close to the 1988 data and visa versa is an irrelevant by-product of displaying all three data sets on the same plot and should be ignored.

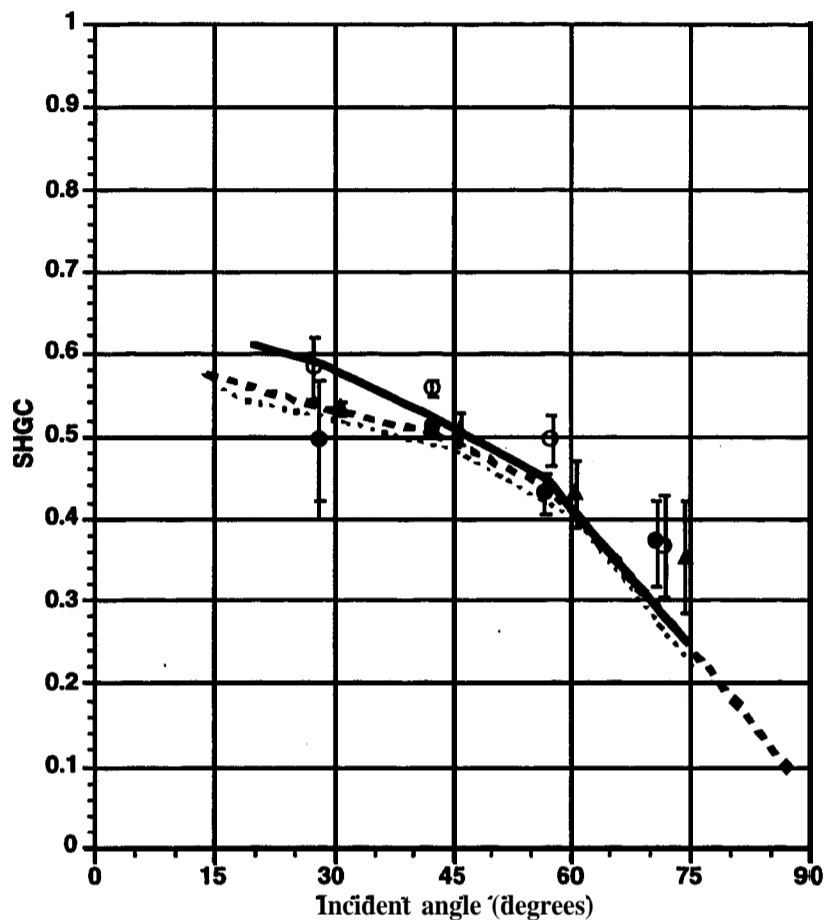


Figure 7. Comparison of the Layer Calculation of *SHGC* with the MoWiTT Measurements for Clear Double Glazing with and Interior Venetian Blind. Three sets of *measured* points from measurement periods with slightly different sun trajectories are shown with their corresponding curves calculated with the layer method: Oct., 1988: Solid circles and heavy solid line; Aug., 1989: Open circles and heavy dashed line; Sept., 1991: Solid triangles and light dotted line.

## DISCUSSION

We consider the layer calculations and the MoWiTT measurements in Figure 7 to be in quite significant agreement. The calculation reproduces the angular trend in the data quite well, with the normalization of the curve matching to within 10% in all cases of importance, and in one of the data sets matching quite closely indeed. Considering the difficulty of arranging the blind tilt

reproducibly in the field (a difficulty exacerbated by other issues that were being investigated simultaneously), one would **scarcely** expect better agreement. Where there are larger deviations between the points and the curves, one expects poorer reliability in either the calculation or the measurement (or both). This occurs at the end of the curve: the small-angle point in each data set occurs near sundown when the solar intensity is low, while at the large-angle end the highest sun angle in each data set may give data of poor quality because of the effects of window reveal and blind edges, which are not dealt with in the calculation. In addition, as discussed in the section on scanner measurements, large errors in the region of  $75^\circ$  incident angle are expectable.

Venetian blinds are expected to be among the most severe tests of the method, and agreement of the angular dependence puts a stringent test on the whole calculation methodology. As indicated in Figure 8, the system front transmittance  $T_{fH}$  and blind layer **absorptance**  $A_{f3}$  ( $A_{fi}$  with  $i=3$ ) in the system have magnitudes that are in some places comparable but have quite different angular shapes. For example, along the line  $\psi = 90^\circ$  going from  $\theta = 30^\circ$  to  $\theta = 0^\circ$ , Figure 5 shows that the SHGC rises slowly, going from around 0.52 to something less than 0.60. But along this same line in Figure 8 the system front transmittance is rising sharply ( $T_{fH}$  goes from about 0.15 to 0.40), while the blind absorptance is falling ( $A_{f3}$  goes from around 0.40 to 0.20). Since the blind inward-flowing fraction is some 86%, both of these make comparable contributions to the solar heat gain coefficient. Matching the **MoWiTT** angular dependence thus does not come about through the trivial domination of a single physical effect (as is true for transmission in unshaded glazings).

That it was possible to extract a reproducible angular-dependent solar heat gain coefficient from the **MoWiTT** data is in itself a remarkable new achievement. Operating in a fixed orientation for any given test (rather than following the sun), the **MoWiTT** both represents a realistic window environment and experiences a variety of sun angle conditions. Operating a calorimeter in this mode has been controversial, and the demonstration that detailed angular information can be disaggregated from the data gives an important new option in fenestration system property measurement.

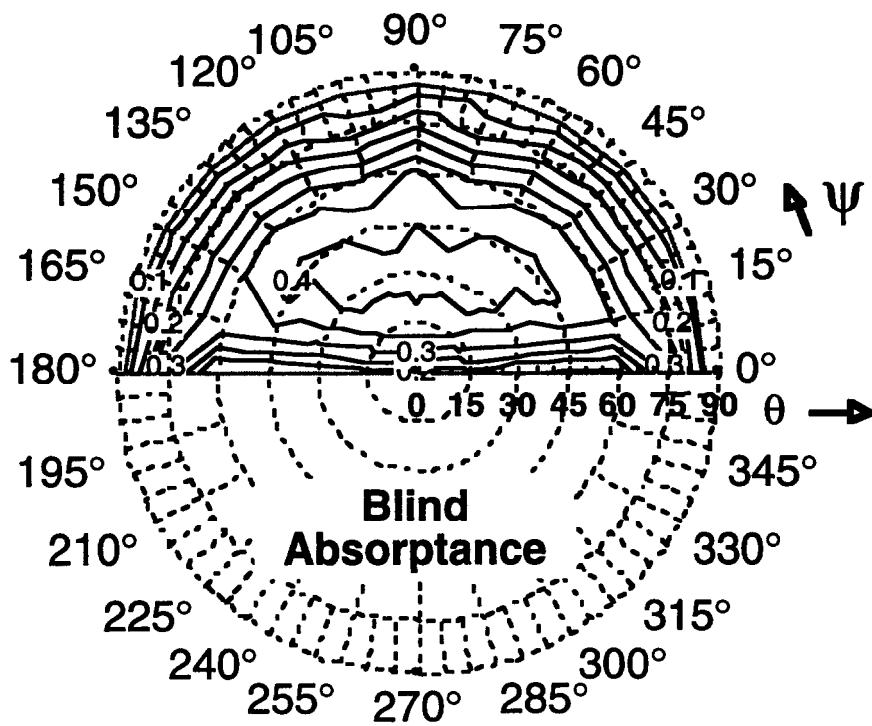
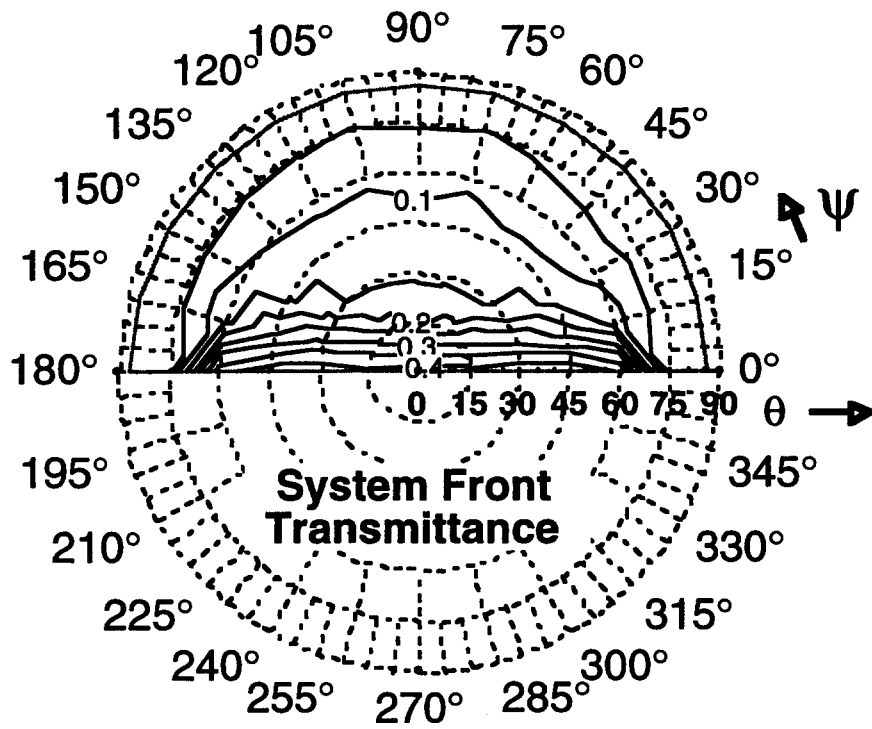


*Figure 8. Contour Plots of the Directional System Front Transmittance and Blind Absorptance in the Sky Half-Hemisphere.*



## CONCLUSIONS

We have demonstrated that the layer calculation method, utilizing scanning photometer measurements, is a viable way of determining the performance of complex fenestration systems, produces data that agrees with the most advanced outdoor calorimeter measurements that have yet been done, and allows the application of a data base incrementally to a wide variety of systems. Accumulating the data base is admittedly an arduous process, but we have now accumulated a set of the most time-consuming measurements--those of inward-flowing-fractions--that should allow the treatment of most of the common systems currently in use.

This makes possible a radically new way of approaching complex fenestrations, where the calorimetry is essentially done and the emphasis is on making the appropriate solar-optical measurements. A considerable variety of methods for making these methods exist or are conceivable, and vary in complexity with the type of system.

The large amount of detailed data produced by the scanner appears to be important for obtaining an accurate characterization of the most optically complex fenestration elements such as venetian blinds. In fact, it appears that a finer angular grid than the 15° one used here may be desirable. Further investigation is warranted to determine the relation between the achievable accuracy and the simplification of measurement.

Further instrumentation work will be necessary to develop a method for dealing with the optical properties of the most complex fenestration elements in a manner that is rapid, accurate and cheap.

This project has not dealt with the question of spectral properties and whether the intermingling of angular and spectral dependence can significantly affect performance. In principle, one would expect this. Research is recommended to explore the practical importance of this issue.

## ACKNOWLEDGMENTS

The authors are grateful for the efforts of Mark **Spitzglas**, who participated in the early stages of scanning radiometer design and construction, of Konstantinos **Papamichael**, who made important contributions to the conceptual and early software development of the project, and of **Ramalingam Muthukurnar**, who assisted in the later development of the analysis software. The efforts of Dennis **DiBartolomeo**, Mary Hinman, Jonathan Slack, and Mehrangiz **Yazdanian** were vital to the completion and automation of the scanning radiometer. Special thanks are due to the **MoWITT** operational team, Carol Ann **Caffrey**, Steve Lambert and Michael **Streczyn**, whose patient and continuous efforts over several years resulted in the inward-flowing fraction measurements. We are indebted to the Experimental Farm, University of Nevada at Reno, for their hospitality in providing a field site and for their cooperation in our activities.

This research was jointly supported by ASHRAE, as Research Project 548-RP under Agreement No. BG 87-127 with the U.S. Department of Energy, and by the Assistant Secretary for Energy Efficiency and Renewable Energy, Office of Building Technologies, Building Systems and Materials Division of the U.S. Department of Energy under Contract No. DE-AC03-76SFOO098.

## REFERENCES

- Klems, J. H. (1988). "Measurement of Fenestration Net Energy Performance: Considerations Leading to Development of the Mobile Window Thermal Test (MoWiTT) Facility." J. Solar Energy Eng. 110:208-216.
- Klems, J. H. (1994A). "A New Method for Predicting the Solar Heat Gain of Complex Fenestration Systems: I. Overview and Derivation of the Matrix Layer Calculation." ASHRAE Trans. 100(pt. 1): 1065-1072.
- Klems, J. H. (1994B). "A New Method for Predicting the Solar Heat Gain of Complex Fenestration Systems: II. Detailed Description of the Matrix Layer Calculation." ASHRAE Trans. 100(pt.1): 1073-1086.
- Klems, J. H. and G. O. Kelley (1995). "Calorimetric Measurements of Inward-Flowing Fraction for Complex Glazing and Shading Systems." ASHRAE Trans. : to be published.
- Klems, J. H., S. Selkowitz, et al. (1982). A Mobile Facility for Measuring Net Energy Performance of Windows and Skylights. Proceedings of the CIB W67 Third International Symposium on Energy Conservation in the Built Environment. Dublin, Ireland, An Foras Forbartha. 3.1.
- Klems, J. H. and J. L. Warner (1992). A New Method for Predicting the Solar Heat Gain of Complex Fenestration Systems. Thermal Performance of the Exterior Envelopes of Buildings V, Clearwater Beach, FL, American Society of Heating, Refrigerating and Air-Conditioning Engineers, Inc.
- Klems, J. H. and J. L. Warner (1995). "Measurement of Bidirectional Optical Properties of Complex Shading Devices." ASHRAE Trans. [to be published in vol 101, pt. 1; Symposium Paper CH-95-8- 1(RP-548)]
- Rubin, M. (1985). "Optical Properties of Soda Lime Silica Glasses." Solar Energy Materials 12: 275-288.